DOI: http://dx.doi.org/10.32571/ijct.1135173 **E-ISSN: 2602-277X**

International Journal of Chemistry and Technology

http://dergipark.org.tr/ijct

Research Article

HOMO–LUMO, NBO, NLO, MEP analysis and molecular docking using DFT calculations in DFPA molecule

Mehmet BAGLAN[1]*, Kenan GÖREN[1], Ümit YILDIKO[2]

[1]*Faculty of Arts and Sciences Department of Chemistry, Kafkas University, Kars, Türkiye*

[2]*Faculty of Engineering and ArchitectureDepartment of Bioengineering, Kafkas University, Kars, Türkiye.*

Received: 14 June 2022; Revised: 31 December 2022; Accepted: 17 May 2023

*****Corresponding author e-mail: mehmetbaglan36@gmail.com

Citation: Baglan, M.; Gören, K.; Yıldıko,Ü. *Int. J. Chem. Technol.* **2023**, 7(1), 38-47

ABSTRACT

Using the Gaussian09 software package, N-(6-(2-(dimethylamino) ethoxy)-5-fluoropyridin-3-yl)-2-(4-fluorophenyl)-5-(trifluoromethyl) pyrazolo[1,5 α]pyrimidine-7-amine(DFPA) the theoretically optimal molecular structure, vibration frequencies and related vibrational movements of the molecule were researched. The DFT(B3PW91 and B3LYP) techniques' 6-311G(d,p) basis set was used to perform quantum chemical computations. HOMO and LUMO analysis were performed for charge transfer in the molecule. NBO analysis was used to examine the stability of the molecule as a result of both charge delocalization and hyperconjugative interaction. DFT approach was used to perform MEP and expected infrared sensitivities and Raman activity are also presented. Geometric parameters of both calculated DFT methods are compatible. Binding affinity values and molecular coupling studies show that the title substance forms a stable complex with MtPanK and PanK. It is possible that the molecule has inhibitory activity against MtPanK and PanK, paving the way for new anti-tuberculosis drugs' the development.

Keywords: DFPA, DFT, MEP, NBO, molecular doking.

DFPA molekülünde DFT hesaplamaları kullanılarak HOMO–LUMO, NBO, NLO, MEP analizi ve moleküler yerleştirme

ÖZ

Gaussian09 yazılım paketi kullanılarak, N-(6-(2-(dimetilamino) etoksi)-5-floropiridin-3-il)-2-(4-florofenil)-5-(triflorometil) pirazolo[1,5-α] pirimidin-7-amin (DFPA) molekülünün teorik olarak optimal moleküler yapısı, titreşim frekansları ve ilgili titreşim hareketleri araştırıldı. Kuantum kimyasal hesaplamaları, DFT (B3PW91 ve B3LYP) yöntemlerinin 6-311G(d,p) temel seti kullanılarak yapılmıştır. Molekül içindeki yük transferini için HOMO ve LUMO analizi yapıldı. Hem hiperkonjugatif etkileşim hem de yük delokalizasyonunun bir sonucu olarak molekülün stabilitesini incelemek için NBO analizi kullanıldı. MEP'i gerçekleştirmek için DFT yaklaşımı kullanıldı ve beklenen kızılötesi duyarlılıkları ve Raman aktivitesi de sunuldu. Hesaplanan her iki DFT yönteminin geometrik parametreleri uyumludur. Bağlanma afinite değerleri ve moleküler eşleşme çalışmaları, başlıktaki bileşiğin MtPanK ve PanK ile stabil bir kompleks oluşturduğunu göstermektedir. Molekülün MtPanK ve PanK'ya karşı inhibitör aktiviteye sahip olması, yeni anti-tüberküloz ilaçlarının geliştirilmesine yol açması mümkündür.

Anahtar Kelimeler: DFPA, DFT, MEP, NBO, moleküler yerleştirme.

DOI: http://dx.doi.org/10.32571/ijct.1135173 E-ISSN: 2602-277X

1.INTRODUCTION

For thousands of years, humanity has been affected by tuberculosis (TB), an extremely contagious disease brought on by Mycobacterium tuberculosis.[1] Tuberculosis has become an epidemic disease that covers the whole world, with 1.4 million fatalities and over 9 million new cases each year.[2] In the next decade, it is estimated that the cost of TB to the least developed countries could be between one and three trillion dollars.[3] Although the global prevalence of TB that is extensively drug-resistant (XDR) and multi-drug-resistant (MDR) has increased dramatically since 1990, the overall number of new cases has decreased by 40%.[4] TB can lay dormant for years after infection, only to resurface when the host's immune system is impaired, such as in HIV co-infected people.[5] Not only has there been significant progress in TB drug discovery recently, but a number of drug candidates have entered various phases of clinical trials.[6] Drug resistor to the existing standard treatment of Mycobacterium tuberculosis (M.tb), known as TB's the causative agent of, is increasing with the discovery of multi-drug resistor TB (MDR-TB) and rifampicin-resistor TB (RR-TB).[7] In 2019, rates of treatment success for drug-sensitive TB were 85%, while for MDR-TB, the rate dropped to 56%.[8] These resistor M.tb stretches require long-term treatment regimens (inclusive injectability) that are more expensive and challenging to obtain. Discovery of new tuberculosis drugs is critical to treat M.tb strains with these resistances.[9] Recently, significant development has been made in new drugs' the development for the treatment of tuberculosis, and many of these agents have been in clinical tests combination therapy's as part.

Density Functional Theory (DFT) is used in theoretical materials research not only to explain material properties, but also to predict entirely new materials with unique properties for a variety of uses.[10] It is done through the use of computational techniques such as Gaussian through DFT calculations.[11] Gaussian is a computer-based application that uses the fundamental principles of quantum mechanics to study the electronic structure of molecules, spectroscopic data, and energies.[12] Quantum calculations including geometry optimization were performed using Gaussian-09 software; Because the software uses a quantum technique, the results are more precise and accurate.[13] Various physicochemical properties can also be calculated using DFT analysis, and also DFT is a low-cost, high-precision computational method for analyzing the electronic structures of molecules used in various scientific fields.[14]

In this study, the B3PW91 and B3LYP methods and the 6-311G(d,p) basis set were used for the theoretical calculation of the DFPA molecule. The charge distribution and quality of the optimized structures of the compounds were determined using NBO analysis. It was possible to visualize and simulate the MEP surface. The polarizability, dipole moment, first-order hyperpolarizability, and thermodynamic characteristics are derived to the title compound. DFT calculations with a base set were also performed to calculate the energy of the Highest Occupied Molecular Orbit (HOMO) and the Least Occupied Molecular Orbit (LUMO). The results of molecular docking studies were conducted to see how the molecules interact with the target binding site of the ligand molecule. Discovered what the minimum binding energy is. Millions of people currently suffer from Mycobacterium tuberculosis, the bacterial cause of tuberculosis. The rise of drug-resistant bacteria has made the search for new antibiotics to fight bacteria a worldwide health priority. The goal of this research was targeted to find new TB drugs by targeting pantothenate kinase, a key enzyme in the universal production of coenzyme CoA.

2. MATERIALS AND METHODS

For DFT calculation, DFT(B3PW91 and B3LYP)/6-311G(d,p) methods were performed bu using Gaussian09 software.[15,16] A quasi-experimental technique is adopted for conformational analysis. The geometry of the resulting molecule was optimized as the computational analysis's the first step. In particular, it requires low energy sensitivity to changes in molecular structure caused by displacement of the core position of DFPA. The DFT method in the Gaussian 09 program was used to calculate the optimum geometries, vibrational frequencies and energies of the molecular structure of DFPA.

The Lee's-Yang-Parr correlation function was created based on the DFT/(B3PW91 and B3LYP) methods and the 6-311G(d,p) base set based program package. Visualization and input file were taken using ChemBio Ultra Drive 3D and GaussView 6.0.16. The binding affinity of the molecule (Maestro Molecular Modeling platform of the Schrödinger, LLC model (version 11.8)) was used to calculate the binding affinity of the molecule. The crystal structure of M. tuberculosis pantothenate kinase (MtPanK) protein (PDB ID: 3AF3) with a resolution factor of 2.35 and the crystal structure of Pantothenate kinase (PanK) protein (PDB ID: 4BFT) with a resolution factor of 2.29 Å were resolved using X-ray diffraction method. Retrieved from the PDB extension file and the RCSB Protein Data Bank (see https://www.rcsb.org/pdb). SDF files from PubChem website for ligand were used separately. It was synthesized with the previous implementation of the Ligprep module. Suspended to prepare protein and retrieve data in the wizard module. Meanwhile, water molecules were separated in a crystal structure. This

DOI: http://dx.doi.org/10.32571/ijct.1135173 E-ISSN: 2602-277X

module of protein ion balance was reconsidered and this time adjusted by selecting active sites due to the flexible binding of the protein. In order to enable flexible insertion by building networks at the protein-binding sites, the receptor meshing module was constructed around mesh boxes. A ligand-protein was inserted using the slip insertion module. Optimal coupling energies were calculated with reference to protein and ligand interactions, alkyl and π interactions, π-π interactions and hydrogen bonds. They provide the highest level of access with the lowest energy configurations. Discovery Studio 4.5 was used to show 2D and 3D interactions as well as the resulting receiver models.

3. RESULTS AND DISCUSSION

3.1. Structure Details and Analysis

Geometric optimization calculations used the B3PW91 vs B3LYP approach with 6-311G(d,p) basis sets for investigate the DFPA molecule effect of the DFT technique on geometric parameters.[17, 18] The most stable optimum geometry parameters determined by DFT of DFPA are shown in Table 1. The largest deviations are between C26–F34 and C1–F7 structures, with bond lengths of 0.00709Å and 0.00655 Å, respectively. Similarly, it was determined that the bond angle between H51–C33–H52 in trihedral structures had the greatest deviation with 0.102987°. It was determined that the bond angle between C25-O28-C29-C30 in tetrahedral structures had the greatest deviation with 1.22219◦. The smallest difference in C5–H37 bond length is -0.00101 Å. The lowest variation in the C15–C14–C17 bond angle is -0.00392◦. The lowest variation in the N12–N11–C16-C15 bond angle is -0.04192.

Table 1. Theoretically obtained some bond lengths (Å) and bond angles (º) of the molecule.

Bond Lengths	B3PW91/ 6-311G(d,p)	B3LYP/ 6-311G(d,p)	Bond Lengths	B3PW91/ 6311G(d,p)	B3LYP/ 6-311G(d,p)
C1-C6	1.38503	1.38648	**C27-H42**	1.08333	1.08217
C3-C4	1.39994	1.40259	**C29-H43**	1.09176	1.09045
C9-C10	1.38847	1.38982	**C33-H51**	1.09025	1.09146
C4-C8	1.46644	1.47034	**C1-F7**	1.34369	1.35024
C14-C17	1.51736	1.52013	**C26-F34**	1.34565	1.35274
C15-C16	1.38615	1.38845	**C17-F19**	1.34130	1.34643
C25-C26	1.40536	1.40695	**C33-N31**	1.45238	1.45893
C29-C30	1.52002	1.52451	**N11-N12**	1.33926	1.34750
C5-H37	1.08415	1.08314	**C23-N24**	1.32602	1.32923
C9-H39	1.07668	1.07577	**C25-O28**	1.34115	1.34595
Bond Angles	**B3PW91/ 6-311G(d,p)**	**B3LYP/ 6-311G(d,p)**	**Bond Angles**	**B3PW91/ 6-311G(d,p)**	**B3LYP/ 6-311G(d,p)**
C1-C6-C5	118.72921	118.70525	**C5-C6-H38**	121.62112	121.64106
C3-C4-C8	120.50005	120.55906	**H51-C33-H52**	107.98561	108.01548
C15-C14-C17	119.38130	119.37738	**C25-O28-C29**	121.01355	121.35501
C16-N21-C22	127.54936	127.72487	**C30-N31-C33**	112.53976	112.62533
C23-N24-C25	120.28953	120.24030	**C14-C17-F18**	111.46092	111.53785
Bond Angles	**B3PW91/ 6-311G**	**B3LYP/ 6-311G(d,p)**	**Bond Angles**	**B3PW91/ 6-311G(d,p)**	**B3LYP/ 6-311G(d,p)**
C3-C4-C8-C9	164.77960	165.07147	**C23-N24-C25-O28**	-179.97602	-179.85731
C16-C15-C14-C17	-178.62637	-178.61233	**C3-C2-C1-F7**	179.96671	179.97025
C25-O28-C29-C30	160.25046	161.47265	**N12-N11-C16-C15**	-178.78116	-178.82308
N13-C14-C17-F18	173.72071	173.73681	**C30-N31-C32-H47**	-175.79271	-175.67547

3.2. Non-Linear Optical Properties (NLO)

Nonlinear optical (NLO) molecules with asymmetric polarization in molecules conjugated to pi-electrons by electron acceptor and electron donor groups can be helpful in computations, telecommunications, and optical signal processing.[19,20] The polarization (α), hyperpolarization (β) and electric dipole moment (μ) of the NLO behavior of DFPA were determined and investigated using the B3PW91/6-311G(d,p) and B3LYP/6-311G(d, p) basis sets.[21,22] In Table 2, values calculated have presented. The criterions for a molecule to function as an efficient NLO is that the first hyperpolarizability (β) is of a large value. A 3x3x3 matrix can be used to describe the first hyperpolarizability, which is a third order tensor. Due to Kleinman symmetry[23] the 3D matrix's 27 components can be broken down into just 10 elements. Equation (1)-(3) gives the mean values of the total first static hyperpolarizability (β), static dipole moment (μ), and polarizability (Δα) of the x, y, and z components. The

DOI: http://dx.doi.org/10.32571/ijct.1135173 E-ISSN: 2602-277X

calculated βtot values of DFPA computed using the DFT/B3PW91/6-311G(d,p) and DFT/B3LYP/6-311G(d,p) method are $3.51x10^{-30}$ esu and $3.57x10^{-30}$ esu, in turn. The calculated dipole moment of the DFPA molecule was computed as 3.6962 and 3.6689 Debye, respectively.

$$\mu = \left(\mu_x^2 + \mu_y^2 + \mu_z^2\right)^{1/2} \quad (1)$$

$$\beta_{Total} = (\beta^2 x + \beta^2 y + \beta^2 z)^{1/2} \quad (2)$$

$$= [(\beta xxx + \beta xyy + \beta xzz)^2 + (\beta yyy + \beta yxx + yzz)^2 + (\beta zzz + \beta zxx + \beta zyy)^2]^{\frac{1}{2}} \quad (3)$$

Table 2. The value of the DFPA molecule belongs to the dipole moments (Debye), polarizability (au), β components and β total value calculated with the 6-311G(d,p) basis set by the DFT/B3PW91-B3LYP method.

Parameters	B3PW91/ 6-311G(d,p)	B3LYP/ 6-311G(d,p)	Parameters	B3PW91/ 6-311G(d,p)	B3LYP/ 6-311G(d,p)
μ x	-2.8386	-2.8082	**β xxx**	-276.5719	-281.3087
μ y	-2.3210	-2.3143	**β yyy**	-18.6724	-17.6063
μ z	0.4657	0.4684	**β zzz**	6.7777	6.6844
μ (D)	3.6962	3.6689	**β xyy**	-33.5448	-36.2407
α xx	-172.8153	-175.8009	**β xxy**	81.9227	87.5145
α yy	-216.3029	-218.7078	**β xxz**	-17.4260	-16.4248
α zz	-194.3745	-195.5322	**β xzz**	-31.4392	-28.4143
α xy	2.0899	2.4043	**β yzz**	19.9700	20.5157
α xz	-3.5615	-3.5036	**β yyz**	15.3104	15.3594
α yz	-2.4141	-2.4376	**β xyz**	2.6743	3.4133
α (au)	-194.4975	-196.6803	**β (esu)**	$3.51x10^{-30}$	$3.57x10^{-30}$

3.3. Mulliken Atomic Charges

Atomic charge has been used to characterize charge transfer and electronegativity equalization in processes as well as to predict the electrostatic potential outside of molecule surfaces.[24, 25] The Mulliken atomic charges computed at B3PW91/6-311G(d,p) and B3LYP/6-311G(d,p) levels for various atoms of DFPA are shown in Table 3. The aromatic ring's negative values of at atoms C2, C4, C5, C14, N11 and N24 cause electron density redistribution. C5 and C27 become more acidic as a result of their strong negative charges, allowing them to harbor higher positive charges. Mulliken, bond angles, atomic masses and structure optimization views of DFPA molecule at B3PW91/6-311G(d,p) and B3LYP/6-311G(d,p) levels are as in Figure 1a.

Table 3. DFT/ B3PW91 and B3LYP techniques with 6-311G(d,p) base sets computed Mulliken atomic charges.

	B3PW91/ 6-311G(d,p)	B3LYP/ 6-311G(d,p)		B3PW91/ 6-311G(d,p)	B3LYP/ 6-311G(d,p)
C1	0.262	0.251	**O28**	-0.327	-0.326
C2	-0.144	-0.126	**N11**	-0.420	-0.374
C4	-0.154	-0.132	**N12**	-0.349	-0.18
C5	-0.046	-0.042	**N24**	-0.331	-0.289
C8	0.303	0.259	**N31**	-0.371	-0.357
C9	-0.317	-0.273	**F7**	-0.227	-0.230
C10	0.504	0.437	**F18**	-0.220	-0.221
C14	-0.125	-0.119	**F34**	-0.218	-0.222
C16	0.635	0.583	**H35**	0.124	0.112
C22	0.006	0.022	**H39**	0.120	0.110
C25	0.357	0.326	**H40**	0.155	0.136
C27	-0.005	-0.003	**H42**	0.157	0.141
C29	-0.021	0.010	**H46**	0.125	0.111
C30	-0.155	-0.115	**H47**	0.098	0.083
C32	-0.216	-0.179	**H49**	0.119	0.105
C33	-0.212	-0.176	**H51**	0.274	0.261

DOI: http://dx.doi.org/10.32571/ijct.1135173 E-ISSN: 2602-277X

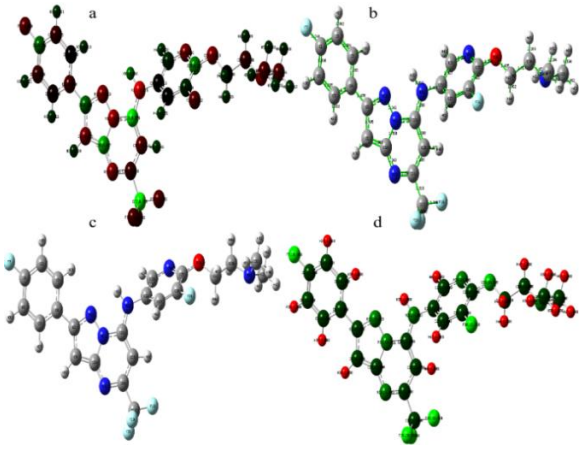

Figure 1. DFPA molecule with DFT/B3LYP/6-311G(d,p) basis set a) mulliken b) bond lengths c) atomic mass d) structure optimization

3.4. HOMO and LUMO Analysis

The terms "Highest Filled Molecular Orbital (HOMO)" and "Lowest Unoccupied Molecular Orbital" are used to express the most fundamental characteristics of quantum chemistry (LUMO).[26] The eigenvalues and energy gaps of the HOMO and LUMO molecules express the molecule's biological activity.[27] A molecule with narrow boundary orbital spacing can be more polarized and has higher chemical reactivity and lower kinetic stability.[28] It is possible to think of the HOMO as the outer orbital holding the electrons, and the ionization potential as being proportional to HOMO energy.[25] Like electron donors, HOMO frequently donates these electrons, so the ionization potential is proportional to the HOMO's the energy.[29] Besides, LUMO can take electrons in and has energy proportional to its affinity for electrons. For the HOMO and LUMO energies, two important molecular orbitals were investigated as shown in Figure 2 and Figure 3.

In Table 4 have calculated quantum chemical parameters (in eV) for low energy compatibilities by DFT/B3PW91/6-311G(d,p)-DFT/B3LYP/6-311G(d,p) methods of the DFPA molecule. Utilizing DFT-based descriptors, chemical potential, spherical stiffness and electrophilicity will guide to understanding the molecule's the structure and reactivity. The electron affinity and ionization energy could be computed by using the orbital energies of LUMO and HOMO as follows: $A=-E_{LUMO}$, $I=-E_{HOMO}$, ($\mu = -(I+A)/2$) and $\eta = (I-A)/2$.[30] This index evaluates the system's energy stability when it receives an additional electronic charge from the environment by calculating the global electrophilic power of a ligand as being equal to = 2/2. A system is said to be electrophilic if it resists exchanging electrons with its surroundings and has the ability to store more electrons than a system that is not.[31] Because it includes information on both stability (hardness) and electron transit (chemical potential), it is a better indicator of overall chemical reactivity. The chemical potential μ and hardness η are determined by the following equations: $\eta = (I-A)/2$ and $\mu = -(I+A)/2$, where, chemical species are the ionization potential (I) and electron affinity(A). Since the chemical potential the title compound's is stable and negative due to this negativity, the elements from which they are formed do not spontaneously decompose.[32] The resistance of an electron cloud in a chemical system to deformation due to slight disturbances during chemical processing is referred to as its stiffness. The concept of hardness is used in physics and chemistry, but it cannot be observed experimentally. Hard systems are less polarized and generally small, although soft systems can be highly and highly polarized.[33]

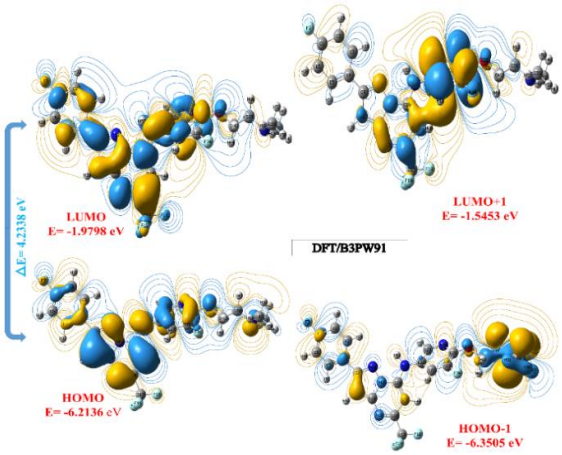

Figure 2. Boundary molecular orbitals of the DFPA compound according to the DFT/B3PW91/6-311G(d,p) level.

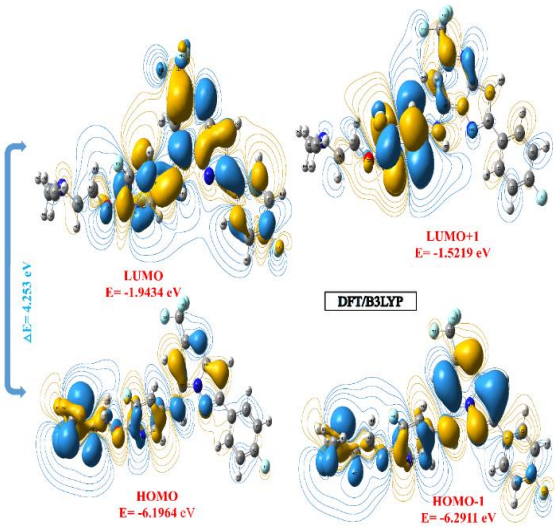

Figure 3. Boundary molecular orbitals of the DFPA compound according to the DFT/B3LYP/6-311G(d,p) level.

DOI: http://dx.doi.org/10.32571/ijct.1135173 E-ISSN: 2602-277X

Table 4. Calculated quantum chemical parameters*(in eV) for low energy compatibilities by DFT/B3PW91/6-311G(d,p)-DFT/B3LYP/6-311G(d,p) methods of the DFPA molecule.

Molecules Energy		DFT/ B3PW91 /6-311G(d,p)	DFT/B3LYP/ 6-311G(d,p)
E_{LUMO}		-1.9798	-1.9434
E_{HOMO}		-6.2136	-6.1964
E_{LUMO+1}		-1.5453	-1.5219
E_{HOMO-1}		-6.3505	-6.2921
Energy Gap	$(\Delta)\lvert E_{HOMO}- E_{LUMO}\rvert$	4.2338	4.2530
Ionization Potential	$(I = -E_{HOMO})$	6.2136	6.1964
Electron Affinity	$(A = -E_{LUMO})$	1.9798	1.9434
Chemical hardness	$(\eta = (I - A)/2)$	2.1169	2.1260
Chemical softness	$(s = 1/2\ \eta)$	1.0584	1.063
Chemical Potential	$(\mu = -(I + A)/2)$	-4.0967	-4.0699
Electronegativity	$(\chi = (1+ A)/2)$	1.4899	1.4717
Electrophilicity index	$(\omega = \mu^2/2\ \eta)$	3.9640	3.8956

3.5. Molecular Electrostatic Potential (MEP)

MEP is a valuable descriptor describing nucleophilic and electrophilic processes, as well as hydrogen bond interactions, and it is connected to electron density (ED).[34] In research procedures requiring the recognition of one molecule by another, such as interactions between drugs and receptors and enzymes and substrates, the electrostatic potential V(r) is ideally suited.[35] Because these two species first see each other through their potential. The nucleophilic and electrophilic regions of the studied molecule were predicted using MEP in optimized geometry by the B3PW91/6-311G,p) and B3LYP/6-311G(d,p) basis sets. Electrophilic reactivity is represented by MEP's negative (red or yellow) portions while nucleophilic reactivity is represented by positive (blue) regions as shown in Figure 4.

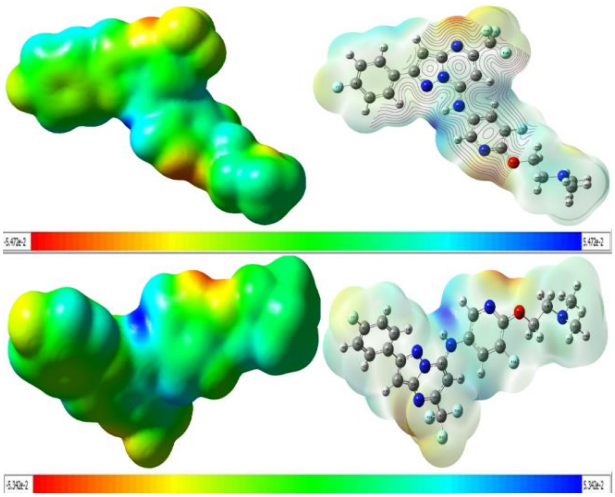

Figure 4. Molecular electrostatic potential surface by DFT/ B3PW91 and DFT/B3LYP methods with 6-311G(d,p) and 6-311G(d,p) basis set.

3.6. NBO Analizi

Conjugative interaction in a molecular system becomes clear with NBO analysis.[36] The stabilization of molecular systems is based on orbital interactions between occupied (donor) and vacant (acceptor) bonding orbitals. For DFPA, a quadratic. The receiver(j) and donor(i) relationship was predicted using Fock marix. This orbital intelligence is capable of both forming and weakening bonds.[37] The stabilizing value associated with delocalization for every donor (i) and recipient (j) is expected to be as follows.

$$E(2) = \Delta Eij = qi\frac{(Fi,j)^2}{(\varepsilon i - \varepsilon j)} \quad (4)$$

Fock matrix NBO element is F(i,j), diagonal elements are Ɛi and Ɛj, and donor orbital occupancy is qi. The higher the stabilization energy, the more likely it is that electrons will be donated to the acceptor orbitals. NBO study of DFPA revealed molecular hybridization, charge density delocalization and conjugative interaction. Table 5 shows the electron density, E(2), E(j)–E(i) and f(i,j) values, as well as NBO calculations for a few selected donors and acceptors. The interaction between the stabilization energy E(2), filled and vacant NBO type Lewis orbitals, and electron delocalization from the bonding (BD) to the

DOI: http://dx.doi.org/10.32571/ijct.1135173 E-ISSN: 2602-277X

antibonding (BD*) orbitals is described using NBO analysis. The more intense the connection between recipients and donors, the higher the E(2) value. Bond (σ/π) and anti-bond (σ*/π*) interactions also contributed significantly to the stability of the structure, with π(C9-C10) /π*(C8-N12) interaction having the highest E(2), followed by π(C15-C16) /π*(N13-C14) with 30.17 kcal/mol. Afterwards, it was determined that the σ (C8-C9)/σ* (C10-N13) interaction had the highest E(2) value with 7.54 kcal/mol.

Table 5. Selected NBO results for DFPA utilizing the B3PW91/6-311G(d, p) theory level to show the generation of Lewis and non-Lewis orbitals

NBO(i)	Type	ED/e	NBO(j)	Type	ED//e	E(2)[a] (Kcal/mol)	E (j)-E(i)[b] (a.u.)	F (i, j)[c] (a.u)
C2-C1	σ	1.98135	**C6-C1**	σ*	0.02824	4.28	1.28	0.066
C6-C1	σ	1.98127	**C2-C1**	σ*	0.02844	4.27	1.28	0.066
C6-C1	π	1.64891	**C3-C2**	π*	0.31928	18.13	0.30	0.066
C1-C6	π	1.64891	**C5-C4**	π*	0.37881	21.44	0.30	0.072
C3-C2	π	1.68221	**C6-C1**	π*	0.37287	23.50	0.28	0.073
C3-C32	π	1.68221	**C5-C4**	π*	0.37881	18.28	0.29	0.066
C2-H35	σ	1.97610	**C4-C3**	σ*	0.02406	4.02	1.08	0.059
C3-C4	σ	1.97137	**C5-C4**	σ*	0.02343	4.30	1.25	0.066
C3-H36	σ	1.97796	**C5-C4**	σ*	0.02343	4.54	1.08	0.062
C5-C4	α	1.97205	**C4-C3**	σ*	0.02406	4.31	1.25	0.066
C5-C4	π	1.64037	**C6-C1**	π*	0.37287	19.76	0.27	0.066
C5-C4	π	1.64037	**C3-C2**	π*	0.31928	21.45	0.28	0.070
C5-C4	π	1.64037	**C8-N12**	π*	0.48673	21.19	0.25	0.067
C6-C5	σ	1.97294	**C1-F7**	σ*	0.03252	4.00	0.97	0.056
C5-H37	σ	1.97864	**C4-C3**	σ*	0.02406	4.41	1.08	0.062
C6-H38	σ	1.97606	**C5-C4**	σ*	0.02343	4.02	1.09	0.059
C9-C8	α	1.97187	**C10-N13**	σ*	0.02329	7.54	1.19	0.085
C8-N12	α	1.98034	**N11-C16**	σ*	0.03782	5.67	1.25	0.075
C8-N12	π	1.83693	**C5-C4**	π*	0.37881	7.70	0.34	0.049
C8-N12	π	1.83693	**C10-C9**	π*	0.41273	10.14	0.33	0.055
C10-C9	π	1.70562	**C8-N12**	π*	0.48673	36.85	0.26	0.091
C10-C9	π	1.70562	**N13-C14**	π*	0.39238	15.41	0.26	0.058
C16-C15	π	1.68460	**N13-C14**	π*	0.39238	30.17	0.29	0.085
C23-C22	π	1.65654	**N24-C25**	π*	0.43824	16.77	0.27	0.062
C23-C22	π	1.65654	**C27-C26**	π*	0.35645	23.02	0.28	0.072
N24-C25	π	1.70897	**C23-C22**	π*	0.36961	26.36	0.32	0.084
C27-C26	π	1.70782	**C23-C22**	π*	0.36961	16.50	0.30	0.064
C27-C26	π	1.70782	**N24-C25**	π*	0.43824	23.57	0.29	0.076

The energy of a hyper conjugative interaction is denoted by a E (2). (stabilization energy).

b The energy disparity between the acceptor and donor NBO orbitals.

The Fock matrix element between the I and j NBO orbitals is called c F(i, j).

3.7. Molecular Docking Studies

Molecular docking is for seeing and interpreting interactions between a ligand and a protein sensor.[38,39] This method of drug design is highly reliable, fast and cost-effective. Docking score of DFPA-MtPanK and DFPA-PanK are shown Table 6. The Schrödinger program was used to carry out molecular insertion studies of molecules synthesized by Pantothenate kinase (MtPanK) from Mycobacterium tuberculosis in complex with 5'-Guanylyl methylene diphosphonate (GMPPCP) and Pantothenate protein. It was discovered in the Protein Data Bank as the crystal structure (PDB ID:3AF3) of pantothenate kinase (MtPanK). Both proteins and ligands were subjected to editing and optimization. Automatic nesting tecnical were used to create the grid and place the parameter files. A grid was created to arrange the xyz coordinates around binding site's of the enzyme. Discovery Studio Visualizer was used to see and understand the embedding outcomes. The insertion score and H-bond interactions were calculated for the compound included in this study. Here, the binding mechanism is fluoro-bonded TYR-235 (6.43 Å), GOL-321 (3.78). ALA-100 (4.27 Å) and LYS-103 (4.93 Å) are hydrogen bonded to conventional hydrogen bonds. LYS-103 (5.49 Å) bonded to hydroxyl, hydrogen bonded to conventional hydrogen bond. VAL-99 (4.90 Å) Pi-Alkyl is attached to the phenyl center, MET-242 (6.50 Å) Pi-Alkyl is attached to the pyrazolone center and PHE-254 (5.63 Å) is Pi-Alkyl is attached to the carbon. ASP-129 (3.88 Å) Pi-Cation, bound to nitrogen. HIS-179 (4.30 Å) is attached to the pyrazolone center. HIS-179 (4.91 Å)

DOI: http://dx.doi.org/10.32571/ijct.1135173 E-ISSN: 2602-277X

and ARG-238 (6.34 Å) Salt Bridge are connected to the center of the phenyl center. VAL-99 (4.09 Å) bound to flora, ASP-129 (5.10 Å), TYR-153 (5.69 Å), ASP-129 (3.83 Å) and TYR-153 (5.80 Å) bound to nitrile group Van der Waals is an example as shown in Figure 5.

Table 6. Docking score of DFPA-MtPanK and DFPA-PanK.

Compound	Docking Score	
	MtPanK (PDB: 3AF3)	**PanK** (PDB: 4BFT)
DFPA	-6.977	-7.096

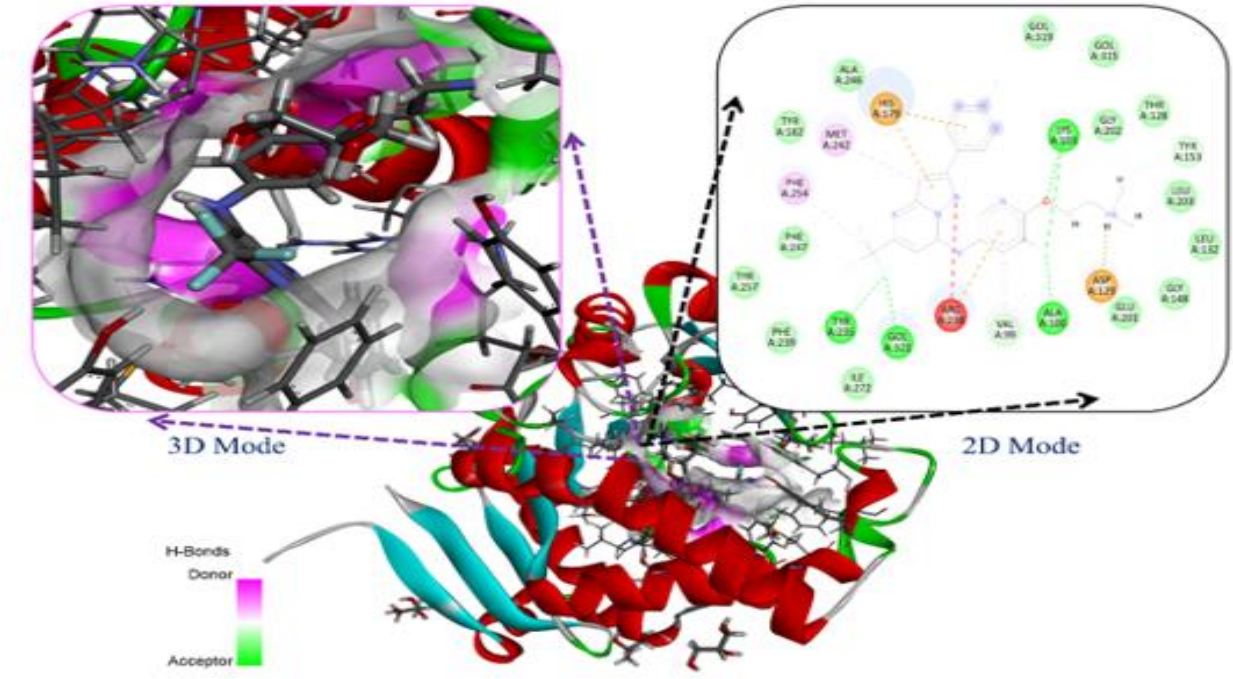

Figure 5. 3D representation of the receptor's aromatic surface and a 2D image of the DFPA-MtPanK enzyme contacts.

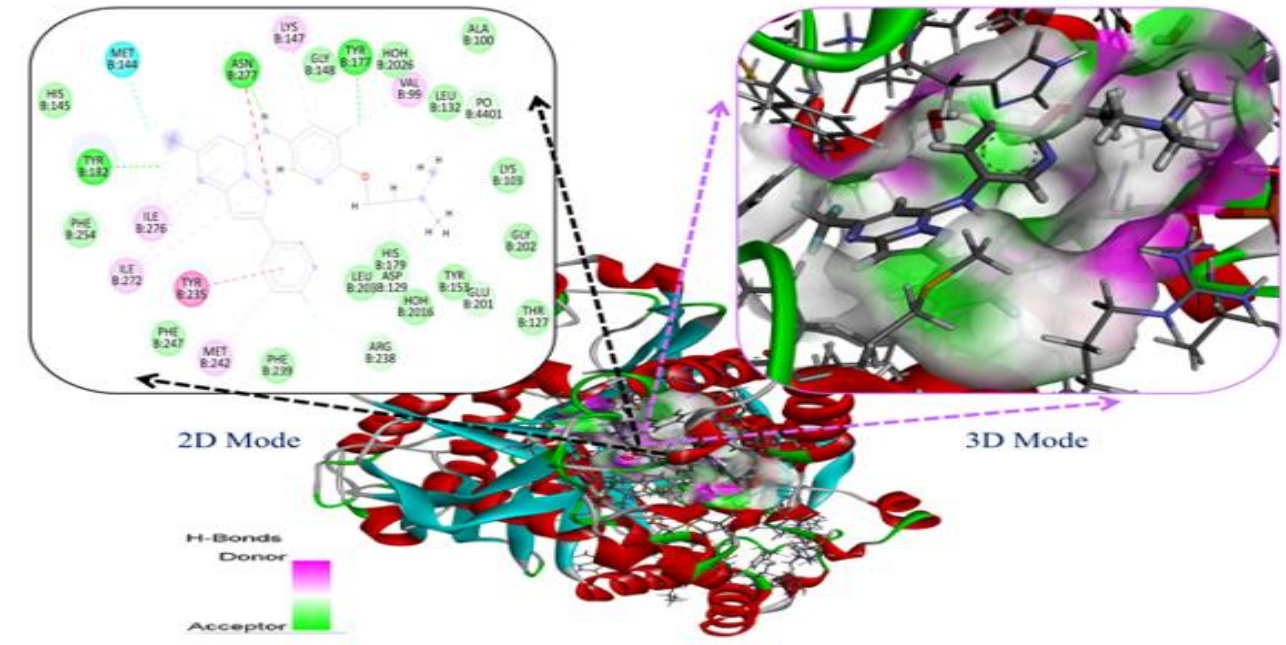

Figure 6. 3D representation of the receptor's aromatic surface and a 2D image of the DFPA-PanK enzyme contacts.

DOI: http://dx.doi.org/10.32571/ijct.1135173 **E-ISSN: 2602-277X**

It was used to conduct molecular docking studies of molecules synthesized by Pantothenate kinase(PanK) from the Crystal structure of Mycobacterium tuberculosis in complex by a triazole inhibitor compound and phosphate protein. Here, the bonding mechanism is TYR-235 (5.82 Å), ASN-277 (5.20 Å) hydrogen bond attached to the conventional hydrogen bond attached to the pyrazolone and LYS-147 (5.05 Å) hydrogen bond attached to the conventional hydrogen bond attached to the nitrile. The TYR-235 (5.57 Å) benzene ring is attached to the center stacked Pi-Pi. META-242 (5.54 Å) Pi-Sulfur bond attached to the center of the benzene ring and PHE-239 (5.56 Å) Pi-Sulfur bond attached to Sulfur. Pi-alkyl bond ARG-238 (6.16 Å) attached to the benzene ring's the center o and ILE-272 (6.04 Å) attached to the pyrazolone ring. ILE-276 (4.44 Å), TYR-182 (5.37 Å), PHE-254 (5.75 Å), and PHE-254 (6.09 Å) are examples of added Alkyl bond as shown in Figure 6.

4. CONCLUSION

The geometry of the optimized molecule was revealed and its molecular parameters, bond length and bond angle were determined. Due to its high hyperpolarizability, the DFPA molecule has strong NLO activity. HOMO-LUMO analysis of the DFPA molecule revealed the compound's the stability and chemical reactivity. In the MEP study, the calculated energy gap and the reactive regions of the investigated molecule demonstrated the compound's the chemical
stability. The stabilization energy by the NBO technique has been used to explain both intramolecular and intermolecular processes. Molecular docking was performed with MtPanK (shift score; -6.977) and PanK (shift score; -7.096) protein receptors, and the best and lowest binding energy obtained was -7.096 Kcal/mol with PanK protein. According to the molecular insertion data, the chemical may have inhibitory activity against MtPanK and PanK, which may lead to the development new anti-tuberculosis drugs's.

Conflict of interests

I declares that there is no a conflict of interest with any person, institute, company, etc.

REFERENCES

1. H.-J. Eun et al., *Biochemical and Biophysical Research Communications,* **2022,** *616*, 19-25.

2. H. Fei et al., *The Lancet Regional Health - Western Pacific,* **2020,** *3*, 100032.

3. M. J. Brennan et al., *Tuberculosis,* **2012,** *92*, S6-S13.

4. A. K. Alame Emane et al *Tuberculosis,* **2021,** *129*, 102092.

5. S. Ashenafi et al., *The American Journal of Pathology,* **2022,** *192* (4), 653-670.

6. S. S . Swain et al., *European Journal of Medicinal Chemistry,* **2022,** *232*, 114173.

7. S. Koirala et al., *Pulmonology,* **2021,** *27* (5), 403-412.

8. Global tuberculosis report 2020. *World Health Organization,* **2020**.

9. P. J . Choi et al., *Tetrahedron Letters,* **2022,** *90*, 153611.

10. M.J. Frisch et al., *Revision, E E.01*.

11. J. I.. Ahamed et al., *Journal of Molecular Structure,* **2022**, 133548.

12. M. Mirnezhad et al., *Journal of Molecular Graphics and Modelling,* **2021,** *104*, 107843.

13. J. Geethapriya et al., *Journal of the Indian Chemical Society,* **2022,** *99* (4), 100418.

14. A. Abdou et al., *Inorganica Chimica Acta,* **2022,** *539*, 121043.

15. M . Sucheta et al., *Materials Today: Proceedings,* **2022**.

16. R. K. Mohapatra et al., *Journal of King Saud University - Science,* **2021,** *33* (2), 101315.

17. N. Kanagathara et al., *Computational and Theoretical Chemistry,* **2021,** *1202*, 113301.

18. S. Budania et al., *Journal of the Indian Chemical Society,* **2022,** *99* (5), 100419.

19. C. Raveendiran et al., *Materials Today: Proceedings,* **2022**.

20. S. Muhammad et al., *Journal of Molecular Graphics and Modelling,* **2022,** *114*, 108209.

21. V. Krishna Kumar et al., *Spectrochimica Acta Part A: Molecular and Biomolecular Spectroscopy,* **2014,** *118*, 663-671.

22. A. S. Karne et al., *Chemical Physics Letters,* **2015,** *635*, 168-173.

23. D. A. Kleinman et al., *Phys. Rev.* **1977-1979.**, 126 (1962).

DOI: http://dx.doi.org/10.32571/ijct.1135173 **E-ISSN: 2602-277X**

24. R. Satheeshkumar et al., *Journal of Molecular Structure*, **2022**, 133552.

25. M. K. Priya et al., *Materials Today: Proceedings*, **2019,** *8*, 37-46.

26. S. Demir aet al., *Journal of Molecular Structure*, **2016,** *1108*, 637-648.

27. K. Sarojini et al., *Molecular and Biomolecular Spectroscopy*, **2012,** *96*, 657-667.

28. E. O. Akintemi et al., *Computational and Theoretical Chemistry*, **2022,** *1210*, 113658.

29. A. T. Tekeş, et al., *Journal of the Institute of Science Tehnology*, **2021,** *11* (4), 2955-2966.

30. N. Jeeva Jasmine et al., *Spectrochimica Acta Part A: Molecular and Biomolecular Spectroscopy*, **2015,** *144*, 215-225.

31. V. Balachandran et al., *Spectrochimica Acta Part A: Molecular and Biomolecular Spectroscopy*, **2013,** *106*, 284-298.

32. R. T. Ulahannan et al., *Spectrochimica Acta Part A: Molecular and Biomolecular Spectroscopy*, **2015,** *151*, 184-197.

33. A. D. Isravel et al., *Computational and Theoretical Chemistry*, **2021,** *1202*, 113296.

34. M. Buvaneswari et al., *Journal of Molecular Structure*, **2021,** *1243*, 130856.

35. R. R. Saravanan et al., *Spectrochimica Acta Part A: Molecular and Biomolecular Spectroscopy*, **2015,** *139*, 321-328.

36. M. A. S . Sakr et al., *Journal of Molecular Structure*, **2022,** *1258*, 132699.

37. A. A. Aboalhassan et al., *Journal of Photochemistry and Photobiology A: Chemistry*, **2022,** *431*, 114039.

38. E. D. Kaya et al., *Journal of Biomolecular Structure and Dynamics*, **2021**, 1-14.

39. R. T. Ulahannan et al., *Spectrochimica Acta Part A: Molecular and Biomolecular Spectroscopy*, **2015,** *150*, 190-199.